J Mol Model (2015) 21:297
DOI 10.1007/s00894-015-2845-4

ORIGINAL PAPER

Substituent effects on the croconate dyes in dye sensitized solar cell applications: a density functional theory study

Ramesh Kumar Chitumalla[1] · **Manho Lim**[2] · **Xingfa Gao**[3] · **Joonkyung Jang**[1]

Received: 10 August 2015 / Accepted: 19 October 2015
© Springer-Verlag Berlin Heidelberg 2015

Abstract Using the density functional theory (DFT), we studied two model croconate dyes, one with an electron-donating substituent (CR1) and the other with an electron-withdrawing group (CR2). The geometric, electronic, and optical properties of these dyes were compared. Upon switching from CR1 to CR2, a considerable bathochromic shift was observed in the electronic absorption spectrum. We also investigated the adsorption behavior of the two dyes on a TiO_2 (101) anatase surface by employing periodic DFT simulations. The periodic electronic-structure calculations revealed that the diketo group of CR1 bound more strongly to the TiO_2 surface than that of CR2, with a binding strength comparable to that of a typical organic D–π–A dye. In this work we evaluate in particular the effect of the electron withdrawing/donating nature of the substituent on the electronic, optical, and adsorption properties of the croconate dyes. Finally, we hope that the present study will help in the design of highly efficient dyes for dye sensitized solar cells by considering substituent effects.

Keywords Croconate · DSSC · TiO_2 · Adsorption · DFT/TDDFT · Periodic DFT

Introduction

As renewable energy devices, dye sensitized solar cells (DSSCs) have attractive features, such as low fabrication cost, light weight, mechanical flexibility, and ease of processing, compared to first and second generation photovoltaic cells [1, 2]. In a standard DSSC, dyes are grafted onto the surface of a wide band gap semiconductor, such as NiO, ZnO, or TiO_2 via anchoring groups, such as carboxylic, sulfonic or phosphonic acids. The semiconductor is in contact with an electrolyte (typically I^-/I_3^- in an organic solvent) and closed by a counter electrode, generally made of Pt [3, 4]. Upon the absorption of light, the ground state dye molecule (S_0) is excited electronically (to S_1), and injects electrons into the conduction band of the semiconductor within a femtosecond lifetime. Subsequently, the dyes are oxidized, and the oxidized dyes, once reaching the ground state, are regenerated by the redox couple present in the electrolyte [5]. The efficiency of DSSCs is affected by a range of factors, such as the energy difference between the excited state of the dye and the conduction band of TiO_2, the grafting of the dye onto the semiconductor (TiO_2), and the properties of the redox couple in the electrolyte [6].

DSSCs employing ruthenium(II) polypyridyl complexes as sensitizers achieve power conversion efficiencies of 11–12 % under standard global air mass 1.5 (AM 1.5G) [5, 7]. The Gr tzel group recently reported a record high conversion efficiency of 13 % using Zn-porphyrin dyes [8]. These metal-based DSSCs, however, are not environmentally friendly and require complicated synthesis and purification processes [9]. On the other hand, metal-free organic dyes have benign environmental effects, high molar extinction coefficients and

Electronic supplementary material The online version of this article (doi:10.1007/s00894-015-2845-4) contains supplementary material, which is available to authorized users.

✉ Joonkyung Jang
jkjang@pusan.ac.kr

[1] Department of Nanoenergy Engineering, Pusan National University, Busan 609-735, Republic of Korea

[2] Department of Chemistry, Pusan National University, Busan 609-735, Republic of Korea

[3] CAS Key Laboratory for Biomedical Effects of Nanomaterials and Nanosafety, Institute of High Energy Physics, Chinese Academy of Sciences, Beijing 100049, China

Published online: 30 October 2015

reasonably cheap preparation processes [10]. The organic D–π–A dyes exhibit 10 % efficiency under AM 1.5G [11]. Several organic dyes, such as coumarins [12–15], merocyanine [16, 17], hemicyanine [18, 19], indoline [20, 21], squaraines [22–26], and croconates [27], are also known to give reasonably good efficiencies.

In particular, croconate dyes, having relatively short backbones containing an oxyallyl subgroup (Fig. 1), can be synthesized easily and give rise to DSSCs that are flexible and interact strongly with light [28, 29]. In addition, croconate dyes have narrow and intense absorption bands in the near infrared (IR) region, and can absorb light even at wavelengths greater than 1100 nm [30, 31]. The near IR absorption of croconate dyes has been attributed to their biradical character [32, 33].

Chemical substitution is an effective method with which to fine tune the absorption and photophysical properties of a dye [10]. Herein, using the density functional theory (DFT), this study showed how chemical substitution on the croconate ring influences the structural, electronic and optical properties of the dye. In particular, the present study investigated two model croconate dyes, CR1 and CR2, with electron-donating (methyl) and -withdrawing (carboxylic acid) substituents, respectively (Fig. 1). We considered COOH as an electron-withdrawing group, instead of NO_2 or CN, as it is the anchoring group most widely employed in DSSC. As an electron-donating group we limited our study to CH_3 and in our future work we are interested to consider more fascinating electron-donating groups such as NH_2. This study also examined how these two different substituents affect the adsorption strength of the diketo groups of CR1 and CR2 to a TiO_2 anatase (101) surface.

Computational details

The DFT/time-dependent DFT (TDDFT) calculations were performed using the Gaussian 09 (G09) *ab initio* quantum chemical software package [34]. The ground state (S_0) optimizations of CR1 and CR2 were performed using the unrestricted hybrid density functional UB3LYP [35–37] and Pople's split valence basis set with polarization and diffuse functions, 6-311+G(d,p). The geometric optimizations were taken to converge when the maximum internal forces acting on all the atoms and the stress were $<4.5\times10^{-4}$ eV/Å and $<1.01\times10^{-3}$ kbar, respectively. The vibrational frequencies were checked to confirm that each configuration is a minimum on the potential energy surface. No symmetry constraints were applied during geometry optimizations.

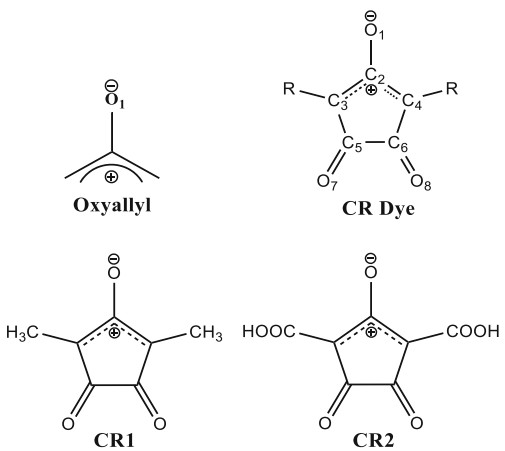

Fig. 1 Structures of the oxyallyl subgroup and the present two model croconate dyes, CR1 and CR2

The adiabatic singlet-triplet gap can be an estimate of the degree of biradical character [32, 38]. For example, Wirz et al. [39] suggested that a molecule can be considered biradical if the splitting between the S_0 and the lowest triplet state T_1, ΔE_{S-T}, falls within 2–24 kcal mol^{-1}. To calculate the singlet-triplet gap (ΔE_{S-T}), the lowest singlet (S_0) geometries were used as the initial geometries for optimizing the T_1 geometries. The T_1 geometries of CR1 and CR2 were obtained at the UB3LYP/6-311+G(d,p) level of theory. The optimized singlet geometries were used to obtain the wave function stability.

The periodic DFT simulation was completed for the adsorption of CR1 or CR2 to a TiO_2 (101) anatase surface using the PWscf code in the Quantum ESPRESSO suite [40]. Geometry optimization was performed using the ultrasoft pseudopotentials of Vanderbilt [41] to describe the electron-ion core interaction. The Perdew-Wang 1991 [42] exchange correlation functional was used for the valence electrons: $2s^2$ and $2p^4$ for oxygen and $3s^2$, $3p^6$, $3d^2$ and $4s^2$ for titanium. The Kohn-Sham orbitals were expanded in a plane-wave basis set with a kinetic energy cutoff of 25 Ry, whereas the augmented density cutoff was expanded to 200 Ry. The Brillouin zone was sampled with a $1\times2\times2$ Monkhorst-Pack k-points [43] mesh. The k-space sampling used in the present study has been used successfully in earlier reports with similar kinds of systems [44, 45]. The Broyden-Fletcher-Goldfrab-Shanno (BFGS) [46] algorithm was used for relaxation of the TiO_2 surface, the CR dyes and CR@TiO_2 complexes.

The anatase (101) surface was modeled as a super cell made from a slab of 24 TiO_2 units. Perpendicular to the slab, i.e., along the surface normal, a vacuum space of 13 Å was placed to prevent unwanted interactions between the periodic slabs. The atomic positions of the bottom layer of the super cell were fixed during structural relaxation. In the case of the TiO_2 surface, the triclinic unit cell had dimensions of a=10.24 Å, b=11.35 Å and c=18.86 Å and contained 72 atoms (see Fig. S1). The adsorption energy (E_{ads}) of a dye to the TiO_2 surface was calculated using the following equation:

$$E_{ads} = E_{Dye@TiO_2} - \left(E_{Dye} + E_{TiO_2}\right),$$

where $E_{Dye@TiO_2}$ is the total energy of the dye@TiO_2 complex, E_{Dye} is the energy of the dye, and E_{TiO_2} is the energy

Table 1 Optimized structural parameters of two model croconate dyes, CR1 and CR2, in the ground state obtained from the UB3LYP/ 6−311+G(d,p) level of theory. Bond distances and angles are in units of Å and degrees, respectively

Dye	O_1-C_2	C_2-C_3/C_2-C_4	C_3-R/C_4-R	C_3-C_5/C_4-C_6	C_5-O_7/C_6-O_8	$O_1C_2C_3/O_1C_2C_4$	$C_3C_2C_4$
CR1	1.229	1.458	1.462	1.468	1.213	128.4	103.3
CR2	1.216	1.465	1.480	1.466	1.208	128.4	103.2

of the TiO_2 surface. A negative value of E_{ads} indicates stable adsorption.

Results and discussion

Molecular structure

Table 1 lists the optimized structural parameters of the two croconate (the optimized CR1 and CR2 structures are drawn in Fig. 2). Previously, the present DFT methods reproduced the experimental geometries of the croconate derivatives [32, 33]. The O_1–C_2 bond length of the oxyallyl subgroup in CR1 was 1.229 Å, which is longer than that of C_5–O_7/C_6–O_8 (1.213 Å). Similarly, in the case of CR2, the O_1–C_2 bond length was 1.216 Å, which longer than that of C_5–O_7/C_6–O_8 (1.208 Å). This suggests that the oxyallyl O_1–C_2 bond has relatively more single bond character than that of C_5–O_7/C_6–O_8. Note that the O_1–C_2 bond in the last two of the three resonance structures of the oxyallyl subgroup is a single bond (see Fig. 3). The positive charge on either C_3 or C_4 in these resonance structures was stabilized in the presence of an electron-donating methyl group. Therefore, the resonance structures with single bond character in the O_1–C_2 bond will be stabilized in CR1. On the other hand, the same resonance structures will be destabilized in CR2 because of the electron-withdrawing (–COOH) substituent. The first resonance structure shown in Fig. 3, where O_1–C_2 is a double bond, will dominate in this case. Therefore, the oxyallyl O_1–C_2 bond in CR1 has larger single bond character than that of CR2. Neither the C_2–C_3/C_2–C_4 nor C_3–C_5/C_4–C_6 bond length varied when the dye was changed from CR1 to CR2. The C_3–R/C_4–R bond length increased considerably by switching from CR1 to CR2. The bond angles of CR1 and CR2 were similar.

Electronic structure and frontier molecular orbitals

Figure 4 shows the frontier molecular orbitals involved in the dominant electron transitions of CR1 and CR2. The highest occupied molecular orbitals (HOMOs) of the two dyes are situated mainly on the diketo groups, and partly on both the central croconate ring and the substituents. The lowest unoccupied molecular orbitals (LUMOs), however, are situated mainly on the central croconate ring and partly on the diketo groups and substituents. The HOMO energies of CR1 and CR2, respectively, are −7.43 and −8.08 eV. The LUMO energies of CR1 and CR2 were found to be −5.07 and −6.06 eV, respectively (Table 2). With the change from CR1 to CR2, the HOMO and LUMO were stabilized by 0.65 and 0.99 eV, respectively. The HOMO–LUMO gap (HLG) values of CR1 and CR2 were 2.36 and 2.02 eV, respectively. The ground state dipole moments (μ_g) of CR1 and CR2 were 2.57 and 1.57 D, respectively (see Table S1 in the supplementary data). The dipole moment decreased considerably (by 1.0 D) as the dye was switched from CR1 to CR2 because of the carboxylic acid substituent.

Singlet (S_0) - triplet (T_1) gaps and biradical character

Oxyallyl is a derivative of trimethylenemethane (TMM)—a biradical species (Fig. S2, the supplementary data) [47]. A previous theoretical study showed that the substitution of one of the methylene groups in TMM by an oxygen atom results in the singlet and triplet states of oxyallyl being almost isoenergetic [48], which has also been confirmed experimentally [49, 50]. The biradical character of TMM is reduced by the substitution of one of the methylene groups with a heteroatom [48]. Fabian and Zahradnik [28, 29] classified such a dye as a biradicaloid dye and attributed

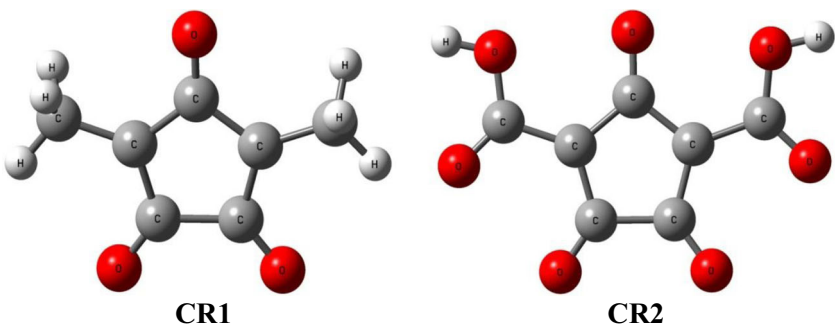

Fig. 2 Optimized geometries of two model croconate dyes CR1 and CR2

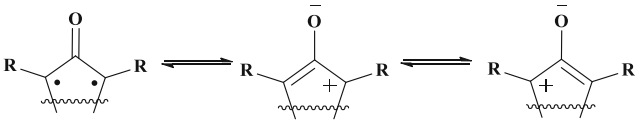

Fig. 3 Resonance structures of the oxyallyl subgroups

the absorption in the near IR region to their biradicaloid nature with a small HLG. Figure S2 (the supplementary data) shows the perturbation of the biradical to the biradicaloid after substituting CH_2 with O.

The singlet state was lower in energy than the triplet state for both CR1 and CR2, confirming that the singlet is the ground state for these dyes. The calculated singlet–triplet gaps were small, suggesting that the present croconate dyes are biradical in nature. Table 2 lists the adiabatic singlet–triplet gaps for the two croconate dyes. The adiabatic singlet–triplet gap decreased with the change from CR1 (10.49 kcal mol^{-1}) to CR2 (2.23 kcal mol^{-1}), indicating the relatively low biradical character of CR1. The wave function stability of the two model croconate dyes was estimated from the analysis

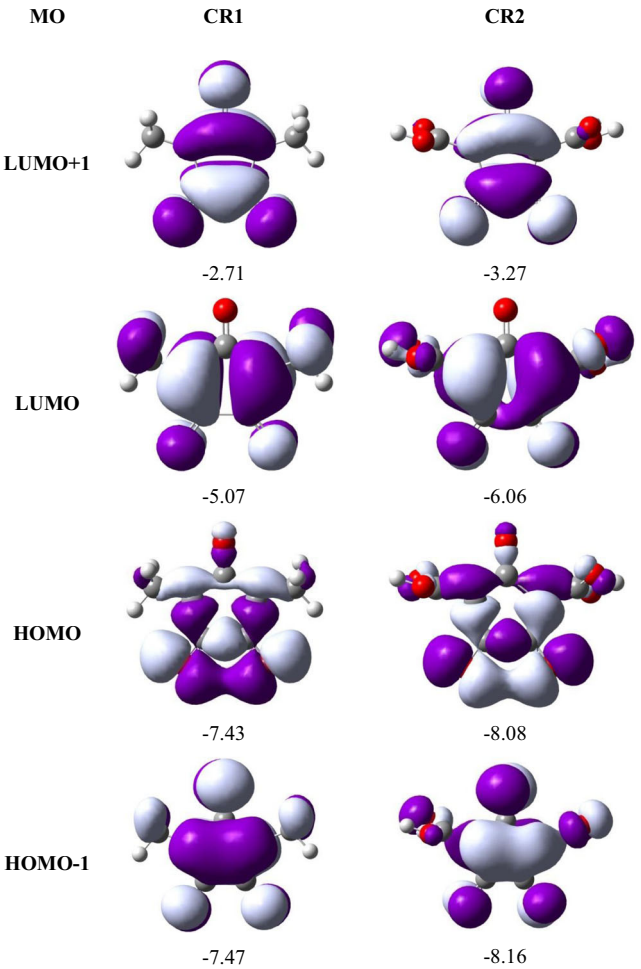

Fig. 4 Computed isodensity (isodensity contour: 0.02 e $Å^{-3}$) surface plots for HOMO−1 to LUMO+1 of CR1 and CR2 at UB3LYP/6-311+G(d,p). Corresponding molecular orbitals (MO) energies (eV) are also given

Table 2 Highest occupied molecular orbital (HOMO), lowest unoccupied molecular orbital (LUMO), and HOMO–LUMO gap (HLG) values along with the singlet−triplet gap (ΔE_{S-T}) and eigenvalue of the stability matrix for dyes CR1 and CR2

Dye	HOMO (eV)	LUMO (eV)	HLG (eV)	[a]ΔE_{S-T} (kcal mol^{-1})	Eigenvalue[b]
CR1	−7.43	−5.07	2.36	10.49	−0.01265
CR2	−8.08	−6.06	2.02	2.23	−0.02535

[a] $\Delta E_{S-T}=E_{Triplet}-E_{Singlet}$

[b] Taken from UB3LYP/6−311+G(d,p) optimized geometries

proposed by Reinhart Ahlrichs [51, 52]. Table 2 presents the wave function stability eigenvalues. A small negative eigenvalue, for both CR1 (−0.01265) and CR2 (−0.02535), indicates mild external instability in the wave function due to the biradical character.

UV-vis absorption spectra

Croconate dyes generally exhibit red to near IR absorption [30, 31, 48], which is a good feature for DSSC applications. The TDDFT was used to understand the nature of the excited states and to examine the vertical excitation energies of the two croconate dyes. Table S1 (supplementary data) lists the present calculations of the electronic transition energies, the transition dipole moments and the oscillator strengths. Figure 5 presents the absorption spectra. The most intense and lowest energy singlet transitions of CR1 and CR2 were observed at 535 and 635 nm, respectively. The major transitions in the low-energy region were assigned to HOMO−1 to LUMO excitation. See the supplementary data (Tables S2 and S3) for the TDDFT data of the first 20 vertical singlet–singlet electronic transitions. A very high bathochromic shift of 100 nm was observed for CR2, which was attributed to the decreased HOMO–LUMO gap and increased biradical character [32, 33] upon substitution of the electron-withdrawing COOH group. The fascinating advantage of croconate dyes is to exhibit their absorption in the red to near IR region. However, the absorption of the two model croconate dyes studied in the present paper did not exceed 700 nm. Here, our main interest is to explore the effect of the substituents on the photophysical properties.

The ground to excited state transition dipole moments (μ_{ge}) for CR1 and CR2 were 4.59 and 4.13 D, respectively. Similar to the trend observed for the ground state dipole moment, the ground to excited state dipole moment also decreased with the change from CR1 to CR2.

Light harvesting efficiencies

The overall conversion efficiency (η) of a DSSC can be calculated from the integral photo-current density (J_{sc}), open-

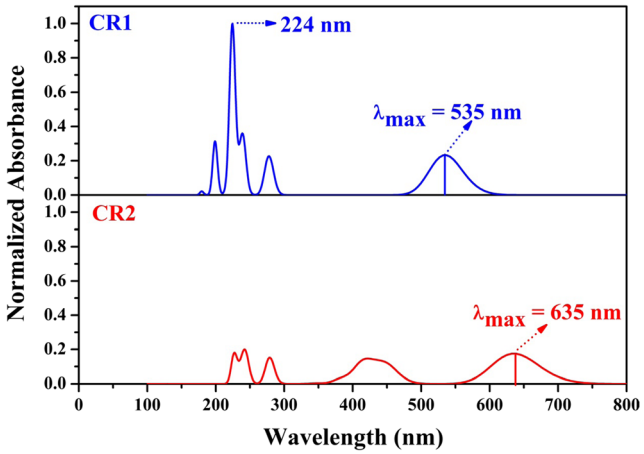

Fig. 5 Simulated UV-vis absorption spectra of CR1 (*top*) and CR2 (*bottom*). The vertical bars represent the oscillator strengths and the spectral lines are broadened by using the Gaussians with full width at half maximum (FWHM)=2000 cm^{-1}

circuit photovoltage (V_{oc}), fill factor of the cell (FF) and the intensity of incident light (I_{ph}), as follows:

$$\eta(\%) = \frac{J_{sc} V_{oc} FF}{I_{ph}} \times 100.$$

Here the J_{SC} can be determined using the following equation [53]:

$$J_{SC} = \int \mathrm{LHE}\ (\lambda)\phi_{\mathrm{inject}}\eta_{\mathrm{collect}}{}^{d\lambda},$$

where LHE (λ), ϕ_{inject}, and η_{collect} are the light harvesting efficiency at a given wavelength, λ, electron injection efficiency and charge collection efficiency, respectively. The LHE (λ) is given by [54].

$$LHE(\lambda) = 1{-}10^{-f},$$

where f denotes the oscillator strength of the sensitizer at a particular wavelength. Generally, an increased LHE value enhances the photocurrent response and thereby the efficiency of the device. The LHE values of CR1 and CR2 calculated at their respective λ_{max} were 0.211 (21.1 %) and 0.164 (16.4 %), respectively (Table S1 in the supplementary data). The LHE value of CR1 was 0.147 larger than that of CR2. Therefore, the dye CR1 is more efficient than CR2 in light harvesting at their corresponding λ_{max}. The calculated LHEs for CR1 and CR2 are moderate at their λ_{max}, but a very high value of LHE (0.620) for the dye CR1 is achieved at 224 nm.

Adsorption of dyes on TiO_2 anatase (101) surface

The binding strength of the CR1 or CR2 to a TiO_2 surface was investigated. Although the rutile form of TiO_2 is thermodynamically more stable, anatase is preferred for DSSC applications because of its relatively large band gap (3.2 eV) and high conduction band energy [10]. The (101) surface, which is the most stable anatase surface, was chosen for simulation [55, 56]. To ensure the consistency and reliability of our adsorption simulation, the adsorption energy of a single water molecule on the TiO_2 surface was calculated. The adsorption energy and geometry of the water molecule on the surface were compared with previous results (see Table S4 and Fig. S3 in the supplementary data). The calculated adsorption energy of water was −12.20 kcal mol^{-1}, which is in excellent agreement with the previous experimental estimates of −11.53 to −16.14 kcal mol^{-1} [44, 45, 57, 58].

An organic D–π–A dye or an organo-metallic ruthenium dye binds to a TiO_2 surface via its carboxylic anchoring groups. On the other hand, the present study considered the adsorption of CR1 or CR2 via its diketo group to the TiO_2 surface. Figure S4 (see supplementary data) presents several plausible configurations of the adsorption. In the monodentate ester type (MET) configuration (a), one keto group participates in the binding. The second configuration (b) is a bidentate chelating (BC), in which only one Ti atom of the slab (Ti_{5C}) binds to both keto groups. In the third configuration (c), called the bidentate bridging (BB), each keto group binds to a five coordinated Ti atom. The BB configuration, which has been shown to be most stable among the three configurations above, was examined [44, 58, 59].

The TiO_2 slab was optimized by imposing the periodic boundary conditions implemented in Quantum ESPRESSO code. The optimized structures of CR1 and CR2 above (from G09) were used for the adsorption studies. The dyes were adsorbed on the TiO_2 in the BB mode and the resulting complexes (dye@TiO_2) were relaxed. Figure 6 shows the optimized structures of the CR1@TiO_2 and CR2@TiO_2 complexes. The C=O bond length of the diketo group for CR1 and CR2 was elongated slightly upon adsorption from 1.21 to 1.25 Å and from 1.20 to 1.24 Å, respectively. This elongation, which is 0.04 Å for both dyes, indicates that the dyes interact strongly with the TiO_2 surface. Figures S5 and S6 show several bond lengths in the optimized geometries of CR1@TiO_2 and CR2@TiO_2 complexes (see supplementary data).

The adsorption energies of CR1 and CR2 were −23.18 and −17.70 kcal mol^{-1}, respectively (Table 3). Therefore, the dye with an electron-donating substituent binds more strongly to the surface than the one with an electron-withdrawing substituent. This is consistent with an earlier report [45] that croconate with an NH_2 substituent binds more strongly to the surface than this dye with a methyl substituent. That is, the adsorption strength increases with increasing electron donating power of the substituent. The enhanced adsorption of CR1 compared to CR2 is also manifested in the fact that the

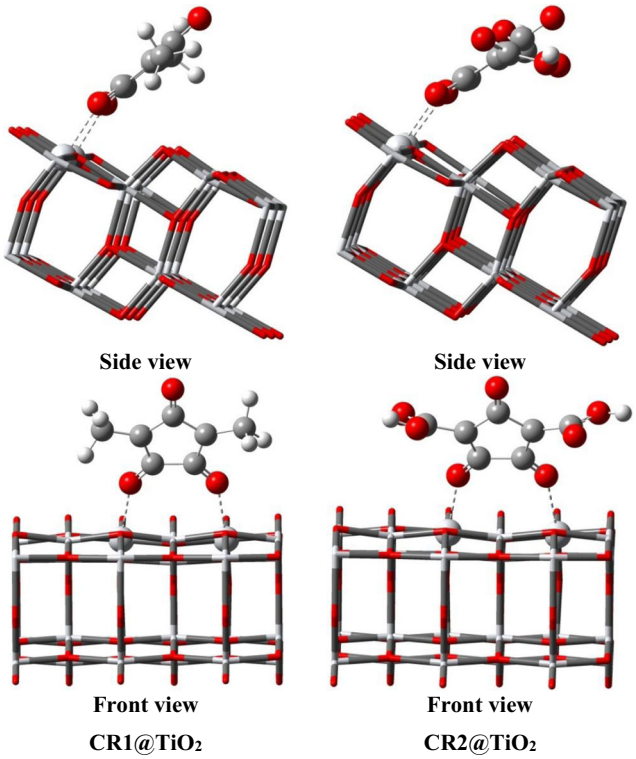

Fig. 6 Adsorption of the diketo groups of CR1 and CR2 in the bidentate bridging mode to the TiO_2 surface

Ti_{5C}–O_7 and Ti_{5C}–O_8 distances of CR1@TiO_2 are smaller than those of CR2@TiO_2. The adsorption energy of the CR1 is comparable to the adsorption energies of several organic D–π–A dyes with COOH anchoring groups [60, 61].

The density of states (DOS) for the clean TiO_2 surface, CR1@TiO_2 and CR2@TiO_2 was calculated (Fig. S7, supplementary data). We also calculated the projected DOS (PDOS) for the dyes. The DOS show broad surface valence and conduction bands separated by a wide band gap (*ca.* 2 eV). Upon adsorption, the dyes develop sharp occupied molecular energy levels in the TiO_2 band gap. The conduction band edge of the TiO_2 surface is shifted by the adsorption but the band gap remains almost the same.

Table 3 Optimized bond lengths and adsorption energies of two model croconate dyes and water molecule to the TiO_2 surface

Dye	Bond lengths (Å)				E_{ads} (kcal mol^{-1})
	C_5–O_7	C_6–O_8	O_7–Ti_{5C}	O_8–Ti_{5C}	
CR1	1.25 (1.21)[a]	1.25 (1.21)[a]	2.26	2.28	−23.18
CR2	1.24 (1.20)[a]	1.24 (1.20)[a]	2.28	2.34	−17.70
H_2O	Ti_{5c}– O_{H_2O}		O_{H_2O} –H		−12.20
	2.29		0.98		

[a] Values given in parentheses are the bond lengths of C_5–O_7/C_6–O_8 before adsorption

Conclusions

Using DFT simulations, the two model croconate dyes with methyl and carboxylic acid substituents, CR1 and CR2, respectively, were investigated systematically. Substituent effects on the structural, electronic, optical, and adsorption properties were studied. The effects of the substituent on the structure of the dye were modest but the optical properties varied significantly depending on the substituent. Periodic DFT calculations showed that the binding energy of the diketo groups of the croconate dye on TiO_2 surface is controlled by the nature of the substituent present on the croconate dye. The binding energy of the croconate dye with CH_3 substitution was significantly higher than that of the dye with COOH substitution. The croconate dye (CR2) had a smaller singlet–triplet gap and a larger biradical character. The higher binding energy and light harvesting efficiency of CR1 compared to CR2 makes it favorable for DSSC applications.

Acknowledgments This study was supported by the National Research Foundation of Korea (NRF) grant funded by the Korea government (MSIP) (Nos. NRF-2014R1A4A1001690 and NRF-2012M3C1A6035363). This work was also supported by the framework of international cooperation program managed by National Research Foundation of Korea (NRF-2014K2A2A2000610).

Compliance with ethical standards

Conflict of interest The authors declare that they have no conflict of interest.

References

1. O'Regan B, Grätzel M (1991) A low-cost, high-efficiency solar cell based on dye-sensitized colloidal TiO_2 films. Nature 353:737–740. doi:10.1038/353737a0
2. Grätzel M (2003) Dye-sensitized solar cells. J Photochem Photobiol C 4:145–153. doi:10.1016/S1389-5567(03)00026-1
3. Nazeeruddin MK, Kay A, Rodicio I, Humphry-Baker R, Mueller E, Liska P, Vlachopoulos N, Graetzel M (1993) Conversion of light to electricity by cis-X2bis(2,2'-bipyridyl-4,4'-dicarboxylate)ruthenium(II) charge-transfer sensitizers (X=Cl-, Br-, I-, CN-, and SCN-) on nanocrystalline titanium dioxide electrodes. J Am Chem Soc 115:6382–6390. doi:10.1021/ja00067a063
4. Heimer TA, Heilweil EJ, Bignozzi CA, Meyer GJ (2000) Electron injection, recombination, and halide oxidation dynamics at dye-sensitized metal oxide interfaces. J Phys Chem A 104:4256–4262. doi:10.1021/jp993438y
5. Nazeeruddin MK, De Angelis F, Fantacci S, Selloni A, Viscardi G, Liska P, Ito S, Takeru B, Grätzel M (2005) Combined experimental and DFT-TDDFT computational study of photoelectrochemical cell ruthenium sensitizers. J Am Chem Soc 127:16835–16847. doi:10.1021/ja0524671
6. Robertson N (2006) Optimizing dyes for dye-sensitized solar cells. Angew Chem Int Ed 45:2338–2345. doi:10.1002/anie.200503083
7. Han L, Islam A, Chen H, Malapaka C, Chiranjeevi B, Zhang S, Yang X, Yanagida M (2012) High-efficiency dye-sensitized solar cell with a novel co-adsorbent. Energy Environ Sci 5:6057–6060. doi:10.1039/c2ee03418b

8. Mathew S, Yella A, Gao P, Humphry-Baker R, CurchodBasile FE, Ashari-Astani N, Tavernelli I, Rothlisberger U, NazeeruddinMd K, Grätzel M (2014) Dye-sensitized solar cells with 13% efficiency achieved through the molecular engineering of porphyrin sensitizers. Nat Chem 6:242–247. doi:10.1038/nchem.1861
9. Feng J, Jiao Y, Ma W, Nazeeruddin MK, Grätzel M, Meng S (2013) First principles design of dye molecules with ullazine donor for dye sensitized solar cells. J Phys Chem C 117:3772–3778. doi:10.1021/jp310504n
10. Hagfeldt A, Boschloo G, Sun L, Kloo L, Pettersson H (2010) Dye-sensitized solar cells. Chem Rev 110:6595–6663. doi:10.1021/cr900356p
11. D Joly, L Pellejà, S Narbey, F Oswald, J Chiron, JN Clifford, E Palomares and R Demadrille (2014) A robust organic dye for dye sensitized solar cells based on iodine/iodide electrolytes combining high efficiency and outstanding stability. Sci Rep 4:4033. doi:10.1038/srep04033
12. Hara K, Kurashige M, Dan-oh Y, Kasada C, Shinpo A, Suga S, Sayama K, Arakawa H (2003) Design of new coumarin dyes having thiophene moieties for highly efficient organic-dye-sensitized solar cells. New J Chem 27:783–785. doi:10.1039/b300694h
13. Hara K, Wang Z-S, Sato T, Furube A, Katoh R, Sugihara H, Dan-oh Y, Kasada C, Shinpo A, Suga S (2005) Oligothiophene-containing coumarin dyes for efficient dye-sensitized solar cells. J Phys Chem B 109:15476–15482. doi:10.1021/jp0518557
14. K Hara, K Sayama, Y Ohga, A Shinpo, S Suga and H Arakawa (2001) A coumarin-derivative dye sensitized nanocrystalline TiO_2 solar cell having a high solar-energy conversion efficiency up to 5.6%. Chem Commun 569–570. doi:10.1039/b010058g
15. Wang Z-S, Hara K, Dan-oh Y, Kasada C, Shinpo A, Suga S, Arakawa H, Sugihara H (2005) Photophysical and (photo)electrochemical properties of a coumarin Dye. J Phys Chem B 109:3907–3914. doi:10.1021/jp044851v
16. Sayama K, Tsukagoshi S, Hara K, Ohga Y, Shinpou A, Abe Y, Suga S, Arakawa H (2002) Photoelectrochemical properties of J aggregates of benzothiazole merocyanine dyes on a nanostructured TiO_2 film. J Phys Chem B 106:1363–1371. doi:10.1021/jp0129380
17. Sayama K, Hara K, Mori N, Satsuki M, Suga S, Tsukagoshi S, Abe Y, Sugihara H, Arakawa H (2000) Photosensitization of a porous TiO_2 electrode with merocyanine dyes containing a carboxyl group and a long alkyl chain. Chem Commun 1173–1174. doi:10.1039/b001517m
18. Chen Y-S, Li C, Zeng Z-H, Wang W-B, Wang X-S, Zhang B-W (2005) Efficient electron injection due to a special adsorbing group's combination of carboxyl and hydroxyl: dye-sensitized solar cells based on new hemicyanine dyes. J Mater Chem 15:1654–1661. doi:10.1039/b418906j
19. Wang Z-S, Li F-Y, Huang C-H, Wang L, Wei M, Jin L-P, Li N-Q (2000) Photoelectric conversion properties of nanocrystalline TiO_2 electrodes sensitized with hemicyanine derivatives. J Phys Chem B 104:9676–9682. doi:10.1021/jp001580p
20. Schmidt-Mende L, Bach U, Humphry-Baker R, Horiuchi T, Miura H, Ito S, Uchida S, Grätzel M (2005) Organic dye for highly efficient solid-state dye-sensitized solar cells. Adv Mater 17:813–815. doi:10.1002/adma.200401410
21. Horiuchi T, Miura H, Sumioka K, Uchida S (2004) High efficiency of dye-sensitized solar cells based on metal-free indoline dyes. J Am Chem Soc 126:12218–12219. doi:10.1021/ja0488277
22. Matsui M, Mase H, Jin J-Y, Funabiki K, Yoshida T, Minoura H (2006) Application of semisquaric acids as sensitizers for zinc oxide solar cell. Dyes Pigm 70:48–53. doi:10.1016/j.dyepig.2005.04.008
23. Alex S, Santhosh U, Das S (2005) Dye sensitization of nanocrystalline TiO_2: enhanced efficiency of unsymmetrical versus symmetrical squaraine dyes. J Photochem Photobiol A 172:63–71. doi:10.1016/j.jphotochem.2004.11.005
24. Qin C, Numata Y, Zhang S, Yang X, Islam A, Zhang K, Chen H, Han L (2014) Novel near-infrared squaraine sensitizers for stable and efficient dye-sensitized solar cells. Adv Funct Mater 24:3059–3066. doi:10.1002/adfm.201303769
25. Prohens R, Portell A, Font-Bardia M, Bauzá A, Frontera A (2014) Experimental and theoretical study of aromaticity effects in the solid state architecture on squaric acid derivatives. Cryst Growth Des 14:2578–2587. doi:10.1021/cg500264k
26. Park J, Barbero N, Yoon J, Dell'Orto E, Galliano S, Borrelli R, Yum JH, Di Censo D, Gratzel M, Nazeeruddin MK, Barolo C, Viscardi G (2014) Panchromatic symmetrical squaraines: a step forward in the molecular engineering of low cost blue-greenish sensitizers for dye-sensitized solar cells. Phys Chem Chem Phys 16:24173–24177. doi:10.1039/c4cp04345f
27. Takechi K, Kamat PV, Avirah RR, Jyothish K, Ramaiah D (2007) Harvesting infrared photons with croconate dyes. Chem Mater 20:265–272. doi:10.1021/cm7018668
28. Fabian J, Zahradník R (1989) The search for highly colored organic compounds. Angew Chem Int Ed 28:677–694. doi:10.1002/anie.198906773
29. Fabian J, Nakazumi H, Matsuoka M (1992) Near-infrared absorbing dyes. Chem Rev 92:1197–1226. doi:10.1021/cr00014a003
30. Langhals H (2003) An unexpectedly simple NIR Dye for 1.1 μm with a central mesoionic structure. Angew Chem Int Ed 42:4286–4288. doi:10.1002/anie.200301642
31. Tian M, Tatsuura S, Furuki M, Sato Y, Iwasa I, Pu LS (2002) Discovery of novel dyes with absorption maxima at 1.1 μm. J Am Chem Soc 125:348–349. doi:10.1021/ja0209666
32. Yesudas K, Bhanuprakash K (2007) Origin of near-infrared absorption and large second hyperpolarizability in oxyallyl diradicaloids: a three-state model approach. J Phys Chem A 111:1943–1952. doi:10.1021/jp068900a
33. Prabhakar C, Yesudas K, Bhanuprakash K, Rao VJ, Santosh Kumar RS, Rao DN (2008) Linear and nonlinear optical properties of mesoionic oxyallyl derivatives: enhanced non-resonant third order optical nonlinearity in croconate dyes. J Phys Chem C 112:13272–13280. doi:10.1021/jp803025v
34. Frisch MJ, Trucks GW, Schlegel HB, Scuseria GE, Robb MA, Cheeseman JR, Scalmani G, Barone V, Mennucci B, Petersson GA, Nakatsuji H, Caricato M, Li X, Hratchian HP, Izmaylov AF, Bloino J, Zheng G, Sonnenberg JL, Hada M, Hada M, Ehara M, Toyota K, Fukuda R, Hasegawa J, Ishida M, Nakajima T, Honda Y, Kitao O, Nakai H, Vreven T, Montgomery JA Jr, Peralta JE, Ogliaro F, Bearpark M, Heyd JJ, Brothers E, Kudin KN, Staroverov VN, Kobayashi R, Normand J, Raghavachari K, Rendell A, Burant JC, Iyengar SS, Tomasi J, Cossi M, Rega N, Millam NJ, Klene M, Knox JE, Cross JB, Bakken V, Adamo C, Jaramillo J, Gomperts R, Stratmann RE, Yazyev O, Austin AJ, Cammi R, Pomelli C, Ochterski JW, Martin RL, Morokuma K, Zakrzewski VG, Voth GA, Salvador P, Dannenberg JJ, Dapprich S, Daniels AD, Farkas O, Foresman JB, Ortiz JV, Cioslowski J, Fox DJ (2013) Gaussian 09, Revision D.01. Gaussian Inc. Wallingford, CT
35. Becke AD (1993) Density-functional thermochemistry. III. The role of exact exchange. J Chem Phys 98:5648–5652. doi:10.1063/1.464913
36. Becke AD (1996) Density-functional thermochemistry. IV. A new dynamical correlation functional and implications for exact-exchange mixing. J Chem Phys 104:1040–1046. doi:10.1063/1.470829
37. Lee C, Yang W, Parr RG (1988) Development of the Colle-Salvetti correlation-energy formula into a functional of the electron density. Phys Rev B 37:785–789. doi:10.1103/PhysRevB.37.785
38. Thomas A, Srinivas K, Prabhakar C, Bhanuprakash K, Rao VJ (2008) Estimation of the first excitation energy in diradicaloid croconate dyes having absorption in the near infra red (NIR): a

DFT and SF-TDDFT study. Chem Phys Lett 454:36–41. doi:10.1016/j.cplett.2008.01.074
39. Wirz J (1984) Spectroscopic and kinetic investigations of conjugated bi radical intermediates. Pure Appl Chem 56:1289–1300. doi:10.1351/pac198456091289
40. Baroni S, Dal Corso A, Gironcoli S, Giannozzi P, Cavazzoni C, Ballbio G, Scandolo S, Chiarotti G, Focher P, Pasquarello A, Laasonen K, Trave A, Car R, Marzari N, Kokalj A http://www.pwscf.org/
41. Vanderbilt D (1990) Soft self-consistent pseudopotentials in a generalized eigenvalue formalism. Phys Rev B 41:7892–7895. doi:10.1103/PhysRevB.41.7892
42. Perdew JP, Wang Y (1992) Accurate and simple analytic representation of the electron-gas correlation energy. Phys Rev B 45:13244–13249. doi:10.1103/PhysRevB.45.13244
43. Monkhorst HJ, Pack JD (1976) Special points for Brillouin-zone integrations. Phys Rev B 13:5188–5192. doi:10.1103/PhysRevB.13.5188
44. Srinivas K, Yesudas K, Bhanuprakash K, Rao VJ, Giribabu L (2009) A combined experimental and computational investigation of anthracene based sensitizers for DSSC: comparison of cyanoacrylic and malonic acid electron withdrawing groups binding onto the TiO2 anatase (101) surface. J Phys Chem C 113:20117–20126. doi:10.1021/jp907498e
45. Puyad A, Kumar C, Bhanuprakash K (2012) Adsorption of croconate dyes on TiO2 anatase (101) surface: a periodic DFT study to understand the binding of diketo groups. J Chem Sci 124:301–310. doi:10.1007/s12039-012-0229-1
46. Fletcher R (1980) Practical methods of optimization, vol 1. Wiley, New York
47. Puyad AL, Prabhakar C, Yesudas K, Bhanuprakash K, Jayathirtha Rao V (2009) High-level computational studies of rhodizonate derivatives: molecules absorbing in near infrared region due to larger C–C–C angle of the oxyallyl ring. J Mol Struct THEOCHEM 904:1–6. doi:10.1016/j.theochem.2009.02.038
48. Prabhakar C, Chaitanya GK, Sitha S, Bhanuprakash K, Rao VJ (2005) Role of the oxyallyl substructure in the near infrared (NIR) absorption in symmetrical dye derivatives: a computational study. J Phys Chem A 109:2614–2622. doi:10.1021/jp044954d
49. Koide T, Furukawa K, Shinokubo H, Shin J-Y, Kim KS, Kim D, Osuka A (2010) A stable non-Kekulé singlet biradicaloid from meso-free 5,10,20,25-tetrakis(pentafluorophenyl)-substituted [26]hexaphyrin(1.1.1.1.1.1). J Am Chem Soc 132:7246–7247. doi:10.1021/ja101040s
50. Ichino T, Villano SM, Gianola AJ, Goebbert DJ, Velarde L, Sanov A, Blanksby SJ, Zhou X, Hrovat DA, Borden WT, Lineberger WC (2009) The lowest singlet and triplet states of the oxyallyl diradical. Angew Chem Int Ed 48:8509–8511. doi:10.1002/anie.200904417
51. Bauernschmitt R, Ahlrichs R (1996) Stability analysis for solutions of the closed shell Kohn–Sham equation. J Chem Phys 104:9047–9052. doi:10.1063/1.471637
52. Bauernschmitt R, Ahlrichs R (1996) Treatment of electronic excitations within the adiabatic approximation of time dependent density functional theory. Chem Phys Lett 256:454–464. doi:10.1016/0009-2614(96)00440-X
53. Zhang J, Li H-B, Sun S-L, Geng Y, Wu Y, Su Z-M (2012) Density functional theory characterization and design of high-performance diarylamine-fluorene dyes with different [small pi] spacers for dye-sensitized solar cells. J Mater Chem 22:568–576. doi:10.1039/c1jm13028e
54. Qin C, Clark AE (2007) DFT characterization of the optical and redox properties of natural pigments relevant to dye-sensitized solar cells. Chem Phys Lett 438:26–30. doi:10.1016/j.cplett.2007.02.063
55. Vittadini A, Selloni A, Rotzinger FP, Grätzel M (1998) Structure and energetics of water adsorbed at TiO_2 anatase 101 and 001 surfaces. Phys Rev Lett 81:2954–2957. doi:10.1103/PhysRevLett.81.2954
56. Vittadini A, Selloni A, Rotzinger FP, Grätzel M (2000) Formic acid adsorption on Dry and hydrated TiO_2 anatase (101) surfaces by DFT calculations. J Phys Chem B 104:1300–1306. doi:10.1021/jp993583b
57. Egashira M, Kawasumi S, Kagawa S, Seiyama T (1978) Temperature programmed desorption study of water adsorbed on metal oxides. I Anatase and rutile. Bull Chem Soc Jpn 51:3144–3149. doi:10.1246/bcsj.51.3144
58. Chitumalla RK, Gupta KS, Malapaka C, Fallahpour R, Islam A, Han L, Kotamarthi B, Singh SP (2014) Thiocyanate-free cyclometalated ruthenium(II) sensitizers for DSSC: a combined experimental and theoretical investigation. Phys Chem Chem Phys 16:2630–2640. doi:10.1039/c3cp53613k
59. Gong X-Q, Selloni A, Vittadini A (2006) Density functional theory study of formic acid adsorption on anatase TiO2(001): geometries, energetics, and effects of coverage, hydration, and reconstruction. J Phys Chem B 110:2804–2811. doi:10.1021/jp056572t
60. Srinivas K, Kumar CR, Reddy MA, Bhanuprakash K, Rao VJ, Giribabu L (2011) D-π-A organic dyes with carbazole as donor for dye-sensitized solar cells. Synth Met 161:96–105. doi:10.1016/j.synthmet.2010.11.004
61. Srinivas K, Sivakumar G, Ramesh Kumar C, Ananth Reddy M, Bhanuprakash K, Rao VJ, Chen C-W, Hsu Y-C, Lin JT (2011) Novel 1,3,4-oxadiazole derivatives as efficient sensitizers for dye-sensitized solar cells: a combined experimental and computational study. Synth Met 161:1671–1681. doi:10.1016/j.synthmet.2011.06.001